Bull. Chem. Soc. Ethiop. **2015**, 29(1), 75-94.
Printed in Ethiopia
DOI: http://dx.doi.org/10.4314/bcse.v29i1.7
ISSN 1011-3924

SPECTROSCOPIC, STRUCTURAL, THERMAL AND ANTIMICROBIAL STUDIES OF 4,6-BIS (4-CHLOROPHENYL)-2-OXO-1,2-DIHYDROPYRIDINE-3-CARBONITRILE WITH SOME TRANSITION METALS

S.A. Sadeek[1*], W.A. Zordok[1], M.S. El-Attar[1] and M.S. Ibrahim[2]

[1]Department of Chemistry, Faculty of Science, Zagazig University, Zagazig, Egypt
[2]Alfa Miser for Industrial Investment, 10th of Ramadan city, Egypt

(Received March 30, 2014; revised September 17, 2014)

ABSTRACT. 4,6-Bis(4-chlorophenyl)-2-oxo-1,2-dihydropyridine-3-carbonitrile (L) reacted with Mn(II), Fe(III), Co(II) and Ni(II) in methanol and acetone as a solvent at room temperature to form a new solid complexes. The isolated complexes were characterized by elemental analysis, magnetic properties, conductance measurements, mass, IR, UV-Vis and ^{1}H NMR spectroscopic methods and thermal analyses. The thermogravimetric and infrared spectroscopic data confirmed the presence of water in the composition of the complexes and the ligand reacted as a bidentate. The metal – ligand binding in metal complexes is predicted using density functional theory. The ligand and their metal complexes were also evaluated for their antibacterial activity. The complexes showed high activities compared with free ligand.

KEY WORDS: Pyridine derivative, 4,6-Bis(4-chlorophenyl)-2-oxo-1,2-dihydropyridine-3-carbonitrile, Transition metal complexes, Antibacterial activity

INTRODUCTION

In recent years the chemistry of heterocyclic compounds are well known for their diverse therapeutic properties and exhibited antibacterial, anticancer, antiulcer, diuretics, anticonvulsant, antihypertensive, antitumor, antifungal, anti-AIDS and antiviral properties [1].

Enones are excellent starting materials for the synthesis of 4,6-bis(4-chlorophenyl)-2-oxo-1,2-dihydropyridine-3-carbonitrile (L) (Scheme 1) via the reaction of enone with ethyl cyanoacetate in the presence of ammonium acetate [2]. However, this procedure is time consuming and gives low yield. Jasinski *et al.* [2, 3] had reported an easy one-step synthesis which gives a higher yield of ligand by heating a mixture of 4-chloroacetophenone, 4-chlorobenzaldehyde, ethyl cyanoacetate and ammonium acetate in presence of glacial acetic acid as a catalyst.

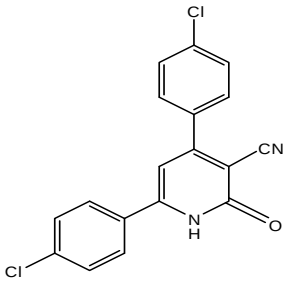

Scheme 1

Metal chelates play an important role in various fields of chemical, biological and technological sciences on coordination; ligands might improve their bioactivity profiles, while

*Corresponding author. E-mail: s_sadeek@zu.edu.eg

some inactive ligand may acquire pharmacological properties. Activity of various anti-inflammatory drugs existing in market has enhanced after complexation with transition metal ion [4].

A detailed literature research has showed that no work is reported on the 4,6-bis(4-chlorophenyl)-2-oxo-1,2-dihydropyridine-3-carbonitrile (L). Thus, our aim was to synthesize and characterize the complexes of Mn(II), Fe(III), Co(II) and Ni(II) with L in order to investigate their magnetic, spectroscopic, thermal and antibacterial properties. Density functional theory (DFT) was used to compute the cation type influence on theoretical parameters of Mn(II), Fe(III), Co(II) and Ni(II) complexes of 4,6-bis-4-chlorophenyl-2-oxo-1,2-dihydropyridine-3-carbonitrile and detect the exact structure of these complexes with different coordination numbers. Profiles of the optimal set and geometry of these complexes were simulated by applying the GAUSSIAN 98W package of programs [5] at B3LYP/CEP-31G [6] level of theory.

EXPERIMENTAL

Reagents and solvents

Reagent grade 4-chloroacetophenone, 4-benzaldehyde, ethyl cyanoacetate, ammonium acetate, glacial acetic acid, ethanol and acetone were purchased from Fluka Chemical Co. $MnSO_4.6H_2O$, $Fe(NO_3)_3.9H_2O$, $CoCl_2.6H_2O$ and $NiSO_4.8H_2O$ from Aldrich Chemical Co. Solvents were purified by standard methods [7].

Preparation of 4,6-bis (4-chlorophenyl)-2-oxo-1,2-dihydropyridine-3-carbonitrile (L)

A mixture of 1,3-bis-(4-chloro-phenyl) propenone (10 mmol), ethyl cyanoacetate (10 mmol) and ammonium acetate (80 mmol) in ethanol (40 mL) was refluxed in the presence of glacial acetic acid for 10 h. After cooling, the precipitate was filtered off, dried and recrystallized from glacial acetic acid to give (L) [3].

Preparation of the metal complexes

The white solid complex $[Mn(L)_2(H_2O)_2]SO_4$ was prepared by adding 0.5 mmol (0.129 g) of manganese sulfate ($MnSO_4.6H_2O$) in 20 mL ethanol drop-wise to a stirred suspended solution 1 mmol (0.340 g) of ligand (L) in 50 mL ethanol. The reaction mixture was stirred for 15 h at 35 ^oC in water bath. The white precipitate was filtered off and dried under vacuum over anhydrous $CaCl_2$. The light yellow, white and light green of $[Fe(L)_2(H_2O)_2](NO_3)_3$, $[Co(L)_2(H_2O)_2]Cl_2$ and $[Ni(L)_2(H_2O)_2]SO_4.6H_2O$ were prepared in similar manner described above by using acetone as a solvent and using $Fe(NO_3)_3.9H_2O$, $CoCl_2.6H_2O$ and $NiSO_4.8H_2O$, respectively, in 1:2 molar ratio.

Elemental C, H and N analysis was carried out on a Perkin Elmer CHN 2400. The percentage of the metal ions were determined gravimetrically by transforming the solid products into metal oxide or sulphate and also determined by using atomic absorption method. Spectrometer model PYE-UNICAM SP 1900 fitted with the corresponding lamp was used for this purposed. IR spectra were recorded on FTIR 460 PLUS (KBr discs) in the range from 4000-400 cm^{-1}. TGA-DTG measurements were carried out under N_2 atmosphere within the temperature range from room temperature to 800 ^oC using TGA-50H Shimadzu thermal analyzer. Electronic spectra were obtained using UV-3101PC Shimadzu spectrophotometer. The solid reflection spectra were recorded with KBr pellets. Mass spectra were recorded on GCMS-QP-2010 plus Shimadzu (ESI-70 eV).

Magnetic measurements were carried out on a Sherwood scientific magnetic balance using Gouy method using $Hg[Co(SCN)_4]$ as calibrant. Molar conductivities of the solution of the ligand and metal complexes in DMF at 1×10^{-3} M were measured on CONSORT K410. All measurements were carried out at ambient temperature with freshly prepared solution.

Antimicrobial investigation

Antibacterial activity of the ligand and its metal complexes was investigated by a previously reported modified method of Beecher and Wong [8] against different bacterial species, such as *Staphylococcus aureus*, *Bacillus subtilis*, *Escherichia coli* and *Pseudomonas aeruginosa* and antifungal screening was studied against two species, *Candida albicans* and *Aspergillus fumigatas*. The tested microorganisms isolates were isolated from Egyptian soil and identified according to the standard mycological and bacteriological keys for identification of fungi and bacteria as stock cultures in the microbiology laboratory, Faculty of Science, Zagazig University. The nutrient agar medium for antibacterial was (0.5% peptone, 0.1% beef extract, 0.2% yeast extract, 0.5% NaCl and 1.5% agar-agar) and Czapek Dox media for antifungal (3% sucrose, 0.3% $NaNO_3$, 0.1% K_2HPO_4, 0.05% KCl, 0.001% $FeSO_4$, 2% agar-agar) was prepared [9] and then cooled to 47 ^oC and seeded with tested microorganisms. Sterile water agar layer was poured, solidified then pour, the prepared growth medium for fungi and bacteria (plate of 12 cm diameter, 15 mL medium plate). After solidification 5 mm diameter holes were punched by a sterile cork-borer. The investigated compounds, i.e. ligand and their complexes, were introduced in Petri-dishes (only 0.1 mL) after dissolving in DMF at 1.0×10^{-3} M. These culture plates were then incubated at 37 ^oC for 20 h for bacteria and for seven days at 30 ^oC for fungi. The activity was determined by measuring the diameter of the inhibition zone (in mm). Bacterial growth inhibition was calculated with reference to the positive control, i.e. ampicilin, amoxycillin and cefaloxin.

RESULTS AND DISCUSSION

4,6-Bis(4-chlorophenyl)-2-oxo-1,2-dihydropyridine-3-carbonitrile (L) complexes of Mn(II), Fe(III), Co(II) and Ni(II) were obtained in moderate good yields (68-78%) as solids of a color characteristics of the metal ion. Single crystals suitable for X-ray crystallographic measurements were not obtained. Table 1 summarizes the carbon, hydrogen and nitrogen elemental analysis as well as melting points and magnetic properties of the isolated solid complexes. The results obtained indicated that all of the isolated complexes are formed from the reaction of the metal salts with L in 1:2 molar ratios. All of the complexes reported here in are hydrates with various degrees of hydration and air stable solids at room temperature. Elemental analyses of C, H, N, S and M (M = Mn, Fe, Co or Ni) are in accordance with the proposed compositions of the complexes. The molar conductivities at room temperature in DMF solvent at 1.0×10^{-3} M of free ligand (L) and their metal complexes were in the range 15.9 to 230.6 S cm^2 mol^{-1} which indicated that the complexes were electrolyte in the solvent with three categories [10]. Conductivity measurements have frequently been used to predicts the structure of metal chelates within the limits of their solubility. They provide a method of testing the degree of ionization of the complexes. It is clear from the conductivity data that the complexes are electrolytes. The obtained results were strongly matched with experimental data which indicated that sulfate, chloride and nitrate groups are found as counter ions (outside the complexes sphere). The magnetic moments (as B.M.) of the complexes were measured at room temperature. The Mn(II), Fe(III), Co(II) and Ni(II) complexes are found in paramagnetism character and octahedral geometry (high spin) around the metal ion with measured magnetic moment values at 5.81, 5.62, 3.72 and 2.73 B.M., respectively.

Table 1. Elemental analysis and physico-analytical data for (L) ligand and its metal complexes.

Compounds M.Wt. (M.F.)	Yield %	Mp °C	Color	Found (calcd.) (%)					μ_{eff}(B.M.)	Λ S cm^2 mol^{-1}
				C	H	N	M	S		
(L) 341 ($C_{18}H_{10}N_2OCl_2$)	80.0	298	White	(63.33) 63.34	(2.91) 2.93	(8.20) 8.21			Diamagnetic	15.9
$[Mn(L)_2(H_2O)_2]SO_4$ 868.93 ($C_{36}H_{24}N_4O_8Cl_4SMn$)	68.5	300	White	(49.69) 49.71	(2.66) 2.67	(6.42) 6.44	(6.32) 6.33	(3.67) 3.68	5.81	190.6
$[Fe(L)_2(H_2O)_2](NO_3)_3$ 959.8 ($C_{36}H_{24}N_7O_{13}Cl_4Fe$)	73.3	288	Light yellow	(44.98) 45.00	(2.49) 2.50	(10.20) 10.21	(4.99) 4.92		5.62	230.6
$[Co(L)_2(H_2O)_2]Cl_2$ 846.9 ($C_{36}H_{28}N_4O_6Cl_6Co$)	69.8	310	White	(49.55) 51.00	(3.27) 3.30	(6.54) 6.61	(6.90) 6.95		3.72	218.8
$[Ni(L)_2(H_2O)_2]SO_4.6H_2O$ 980.8 ($C_{36}H_{30}N_4O_{11}Cl_4SNi$)	78.7	>360	Light green	(43.95) 44.04	(3.00) 3.05	(5.58) 5.70	(5.95) 5.98	(3.22) 3.26	2.73	185

IR absorption spectra

The mid infrared spectra of $[Mn(L)_2(H_2O)_2]SO_4$, $[Fe(L)_2(H_2O)_2](NO_3)_3$, $[Co(L)_2(H_2O)_2]Cl_2$, $[Ni(L)_2(H_2O)_2]SO_4.6H_2O$ and L were measured as KBr discs (Figure 1). The proposed structure for all complexes is represented by Scheme 2

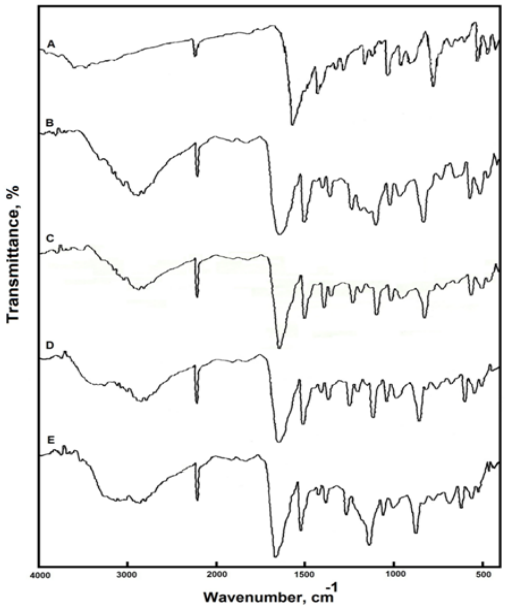

Figure 1. Infrared spectra for (A) (L), (B) $[Mn(L)_2(H_2O)_2]SO_4$, (C) $[Fe(L)_2(H_2O)_2](NO_3)_3$, (D) $[Co(L)_2(H_2O)_2]Cl_2$ and (E) $[Ni(L)_2(H_2O)_2]SO_4.6H_2O$.

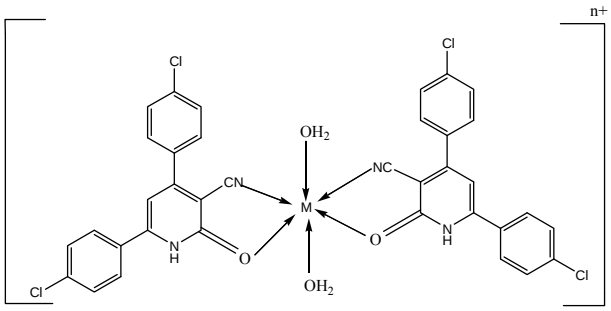

M = Mn(II), Fe(III), Co(II) and Ni(II); n = 3 for Fe(III) and 2 for Mn(II) , Co(II) and Ni(II)

Scheme 2. The coordination mode of M with L.

The four donor atoms of the two ligands (L) coordinated to central metal ions equatorially in a plane forming tetragon with the two oxygen atoms of the two coordinated water molecules axial. According to the proposed structure for the complexes under investigation, the complexes possess a two-fold axis and two planes of symmetry and hence they are C_{2v} symmetry. The C_{2v} complexes, $[M(L)_2(H_2O)_2]^{n+}$ are expected to display 213 vibrational fundamentals which all are monodegenerate and distributed between A_1, A_2, B_1 and B_2 motions; all are IR and Raman active, except A_2 modes which are only Raman active.

The infrared spectrum of free ligand (L) shows two bands at 2215 and 1628 cm^{-1} (Table 2) which are attributed to the stretching vibration of ν(C≡N) for carbonitrile group and ν(C=O) keto group [11, 12]. Upon comparison of the IR spectra of the complexes with that of free ligand the change in intensity of ν(C≡N) from medium to strong (Table 2) confirming that the L molecule coordinated to metal ion through carbonitrile nitrogen. Also, the shift of ν(C=O) to higher frequency value (1636 cm^{-1}) in the spectra of the complexes may indicate an increase of the C=O bond strength upon coordination. The possibility that the electron density on the oxygen atom is decrease upon coordination to metals means decrease in the electron repulsion between the oxygen lone pair and the double bond electrons leading to a stronger C=O bond and then a higher bond frequency. The increase of ν(C=O) frequency upon coordination was reported by the other workers in the spectra of other complexes [13, 14]. These changes of the IR spectra suggest that the free ligand is coordinated to the metal ions via oxygen of keto group and nitrogen of carbonitrile group.

The bands in the range 3533-3378 cm^{-1} in the spectra of the complexes can be attributed to the ν(O-H) vibration of the water molecules [15]. The ν(N-H) vibration appears in the region of 3289-3267 cm^{-1} and the stretching vibrations ν(C-H) of phenyl groups are assigned as a number of bands in the region 3136–3017 cm^{-1} [16].

The spectra of the isolated solid complexes showed a group of new bands with different intensities which characteristics for ν(M-O) and ν(M-N). The *ν*(M-O) band observed at 622, 620, 622 and 633 cm^{-1} for Mn(II), Fe(III), Co(II) and Ni(II), respectively and ν(M-N) found at 467 cm^{-1} with different intensities for Mn(II), Fe(III), Co(II) and Ni(II) complexes indicating coordination of metal ion to ketonic oxygen and carbonitrile nitrogen atoms [17].

Table 2. Infrared frequencies (cm^{-1}) and tentative assignments for (A) L, (B) $[Mn(L)_2(H_2O)_2]SO_4$, (C) $[Fe(L)_2(H_2O)_2](NO_3)_3$, (D) $[Co(L)_2(H_2O)_2]Cl_2.2H_2O$ and (E)$[Ni(L)_2(H_2O)_2]SO_4.6H_2O$.

A	B	C	D	E	Assignments
	3533 mbr	3444 mbr	3378 mbr	3466 mbr	νH_2O
3278 w	3289 w	3289 sh	3283 w	3267 sh	ν(N-H)
3130 w 3088 w 3017 w	3133 w 3089 vw 3020 w	3133 w 3089 sh 3020 w	3133 sh 3089 sh 3020 w	3136 sh 3111 sh 3024 sh	ν(C-H); aromatic
2215 m	2214 s	2214 s	2214 s	2214 s	ν(C≡N)
1628 s	1634 vs	1634 vs	1634 vs	1634 vs	ν(C=O)
1566 sh 1491 ms 1423 vw 1390 w 1346 m	1545 sh 1493 s 1422 w 1389 m 1346 ms	1545 sh 1493 s 1422 sh 1385 m 1346 w	1545 sh 1489 s 1433 sh 1389 w 1346 m	1544 sh 1493 s 1433 sh 1389 w 1346 m	ν(C=C); and phenyl breathing modes and ν_{as}(N-O); NO_3^-
1223 m 1180 w	1223 ms 1178 w	1223 m 1180 m	1223 m 1180 w	1123 s 1178 sh	ν(C-C)
1086 ms 1010 m 957 mbr 818 s 781 sh	1092 s 1011 ms 961 m 822 s 789 sh	1088 s 1011 m 957 w 822 s 790 sh	1088 s 1011 m 956 m 822 s 783 w	1092 s 1011 m 957 w 822 s 787 w	-CH; bending phenyl, $\nu(SO_4^{-2})$ and ν_s(N-O); NO_3^-
717 w 681 vw 642 w 560 s 502 m 453 mbr 437 w	725 m 689 vw 645 m 622 563 s 505 ms 467 s 433 sh	725 w 689 sh 644 w 620 563 m 502 m 467 w 433 sh	725 w 689 sh 644 w 622 563 m 505 w 467 w 433 sh	725w 689 sh 633 m 563 m 502 w 467 w 433 sh	ν(M-O); ν(M-N); ring deformation and $\delta_b(SO_4^{-2})$

Key: s = strong, w = weak, v = very, m = medium, br = broad, sh = shoulder, ν = stretching, δ_b = bending.

UV–Visible solid reflection spectra

The formation of the ligand and its metal complexes was also confirmed by the electronic solid reflection spectra in the range 200-800 nm (Figure 2). The free ligand reflects at 208, 279, 322 and 344 nm, respectively (Table 3) that may be attributed to π-π^* and n-π^* transitions which occur in unsaturated hydrocarbons containing ketonic groups [18]. On complexation, The 208 nm is absent besides a bathochromic shift of the 279, 322 nm bands and the appearance of new reflections. The complexes have bands in the range from 518 to 522 nm which may be assigned to ligand to metal charge-transfer [19]. Also, the presence of new bands in the range of 569 to 682 nm in all complexes may be attributed to d-d transition.

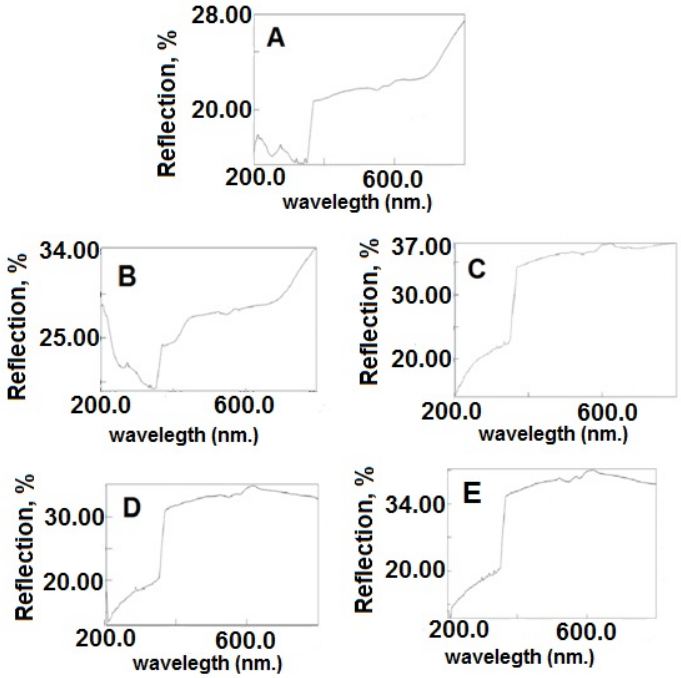

Figure 2. Electronic reflection spectra for (A) 4,6-bis (4-chlorophenyl)-2-oxo-1,2-dihydro-pyridine-3-carbinitrile (L), (B) $[Mn(L)_2(H_2O)_2]SO_4$, (C) $[Fe(L)_2(H_2O)_2](NO_3)_3$, (D) $[Co(L)_2(H_2O)_2]Cl_2$ and (E) $[Ni(L)_2(H_2O)_2]SO_4.6H_2O$.

Table 3. UV-Vis spectra of L and its metal complexes.

Assignments (nm)	L	L_2 complex with			
		Mn(II)	Fe(III)	Co(II)	Ni(II)
π-π^* transitions	208	-	-	-	-
n-π^* transitions	279, 322, 344	271	327, 336	300	299, 319, 325
Ligand-metal charge transfer	-	518	519	522,	522
d-d transition	-	571	569, 620, 672	570, 616, 682	570, 616, 661

^{1}H NMR spectra

The formation of the metal complexes was also confirmed by ^{1}H NMR spectra (Figure 3). The ^{1}H NMR spectra for complexes exhibit new peaks in the range 3.17-3.39 ppm, (Table 4) due to the presence of water molecules in the complexes [1]. Also, the compounds showed peacks in the range δ: 12.85-12.93 for NH amide and at 6.66-8.11 ppm for –CH aromatic. On comparing main peaks of free ligand with its complexes, it is observed that all the peaks of the free ligand are present in the spectra of the complexes with chemical shift upon binding of free ligand to the metal ion [20].

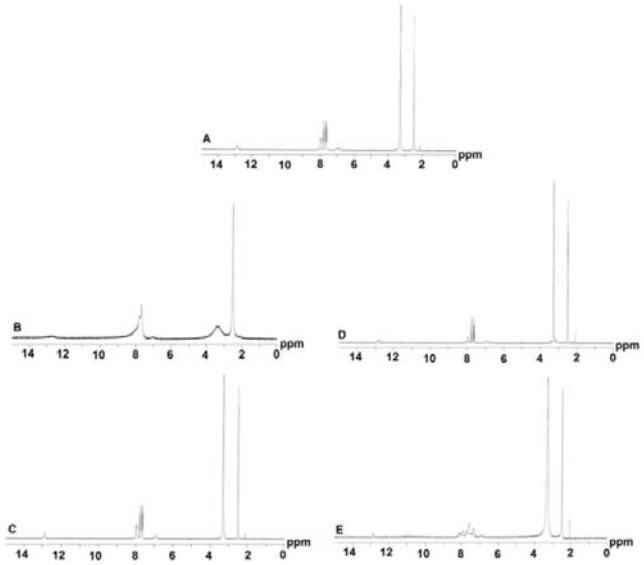

Figure 3. ^{1}H NMR spectra for (A) 4,6-bis (4-chlorophenyl)-2-oxo-1,2-dihydropyridine-3-carbinitrile (L), (B) $[Mn(L)_2(H_2O)_2]SO_4$, (C) $[Fe(L)_2(H_2O)_2](NO_3)_3$, (D) $[Co(L)_2(H_2O)_2]Cl_2$ and (E) $[Ni(L)_2(H_2O)_2]SO_4.6H_2O$.

Table 4. ^{1}H NMR values (ppm) and tentative assignments for (A) (L), (B) $[Mn(L)_2(H_2O)_2]SO_4$, (C) $[Fe(L)_2(H_2O)_2](NO_3)_3$, (D) $[Co(L)_2(H_2O)_2]Cl_2$ and (E) $[Ni(L)_2(H_2O)_2]SO_4.6H_2O$.

A	-	6.88-8.0	12.90
B	3.34	6.66-7.98	12.85
C	3.30	6.90-7.96	12.93
D	3.17-3.39	6.83-7.93	12.87
E	3.30	6.90-8.11	12.86
Assignments	δH, H_2O	δH, -CH aromatic	δH, -NH amide

Mass spectra

Mass spectrum of the free ligand (L) is in a good agreement with the suggested structure. The ligand (L) showed molecular ion peak (M^{+}) at m/z = 340 (24%) and M^{+2} at m/z = 342 (8%) (Figure 4). The molecular ion peak [a] losses Cl_2 to give fragment [b] at m/z = 270 (7%), also it losses Cl^- to give fragment [c] at m/z = 305 (11%), also it losses CN to give fragment [d] at m/z = 314 (8%) and it losses O^-, $C_{12}H_8Cl_2CN$ and $C_{12}H_8Cl_2O$ to give fragment [e] at m/z = 324 (10%), [f] at m/z = 92 (23%) and [g] at m/z = 86 (35%). The molecular ion peak [a] losses $C_{12}H_8Cl_2$ to give fragment [h] at m/z = 118 (11%) and it also losses C_6H_4CNCl to give fragment [i] at m/z = 216 (10%). It losses C_6H_4Cl to give [j] at m/z = 229 (9%) and losses C_6H_4ClO to give fragment [k] at m/z = 213 (23%) (Scheme 3). The fragmentation patterns of our studied complexes were obtained from the mass spectra. The mass spectra of Mn(II), Co(II) and Ni(II) displayed molecular peak at m/z = 868 (17%), 846 (12%) and 980 (29%), respectively, suggesting that the molecular weights of the assigned products matching with elemental and thermogravimetric analyses. Fragmentation pattern of the complex $[Fe(L)_2(H_2O)_2](NO_3)_3$ is used as an example. The molecular ion peak [a] appeared at m/z = 957 (32%) losses $C_{24}H_{16}Cl_4$ to give

[b] at m/z = 513 (22%) and it losses $C_{24}H_{16}Cl_4NO_3$ to give [c] at m/z = 451 (13%). The molecular ion peak [a] losses $(NO_3)_3$ to give [d] at m/z = 771 (12%) and it losses $C_{24}H_{16}Cl_4(NO_3)_2$ to give [e] at m/z = 389 (16%). The molecular ion peak [a] losses $(NO_3)_2$ to give fragment [f] at m/z = 833 (32%) and it losses NO_3 to give fragment [g] at m/z = 895 (11%). The molecular ion peak [a] losses $C_{24}H_{16}Cl_4(NO_3)_3$ to give fragment [h] at m/z = 327 (16%) and it losses $C_{12}H_8Cl_2(NO_3)_3$ to give fragment [i] at m/z = 594 (19%). The molecular ion peak [a] losses $2Cl_2$ to give fragment [j] at m/z = 817 (11%), it losses $C_{12}H_8Cl_2$ to give fragment [k] at m/z = 735 (9%), it losses Cl_2 to give fragment [l] at m/z = 887 (17%) and it losses $C_{12}H_8Cl_2NO_3$ to give fragment [m] at m/z = 611 (20%) (Scheme 4).

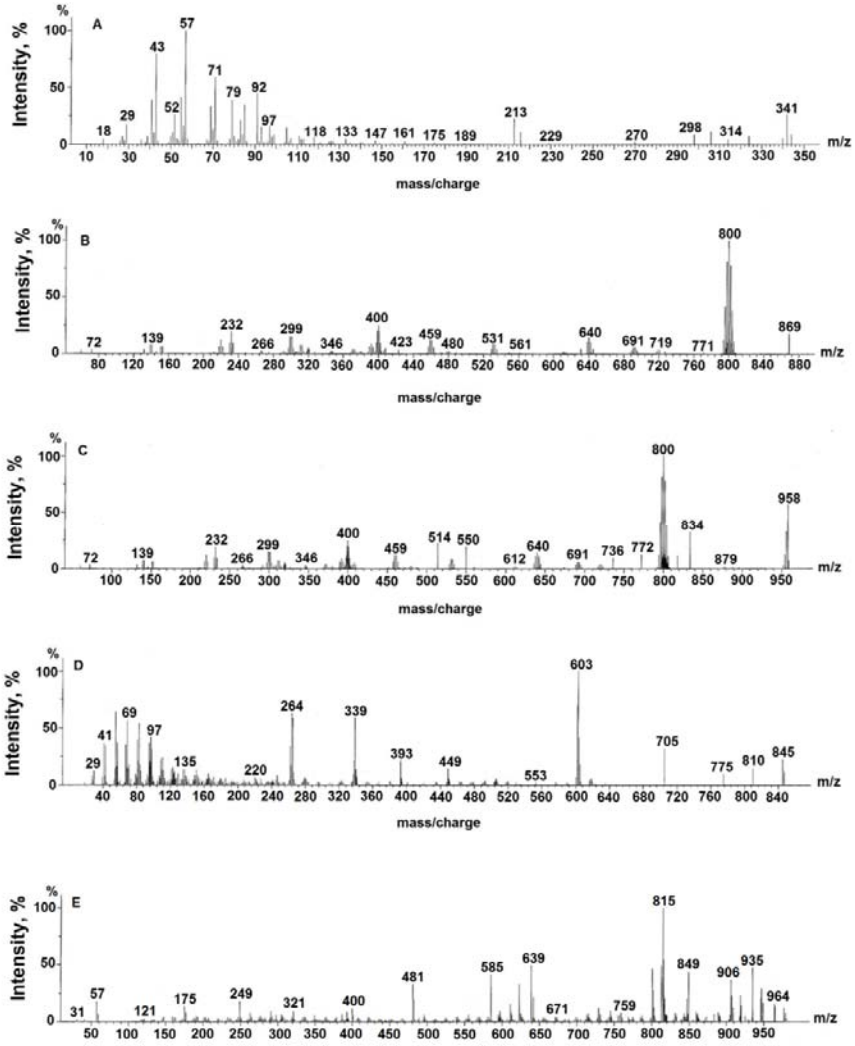

Figure 4. Mass spectra of (A) L, (B) $[Mn(L)_2(H_2O)_2]SO_4$,(C) $[Fe(L)_2(H_2O)_2](NO_3)_3$, (D) $[Co(L)_2(H_2O)_2]Cl_2$ and (E) $[Ni(L)_2(H_2O)_2]SO_4.6H_2O$.

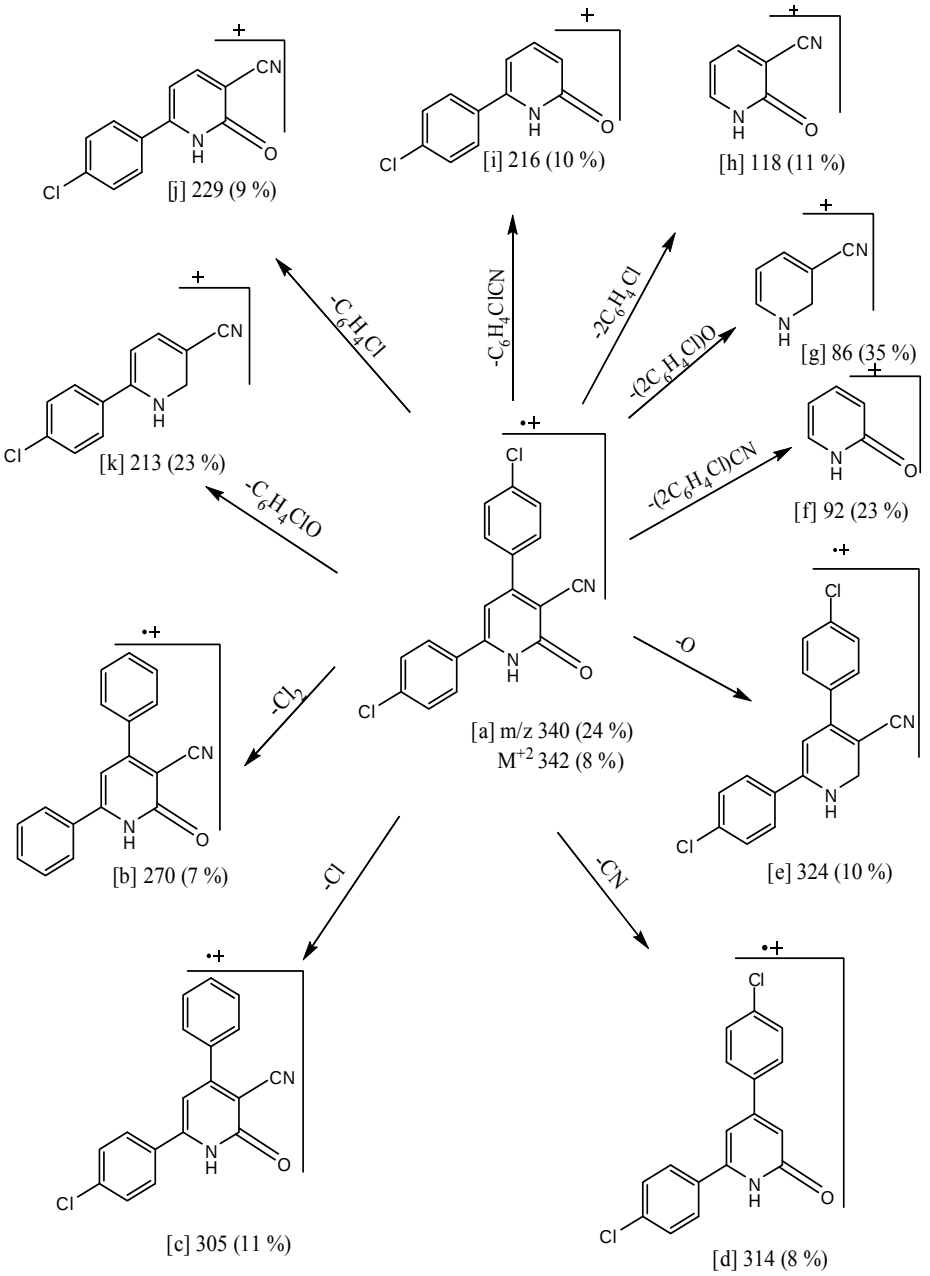

Scheme 3. Fragmentation pattern of L.

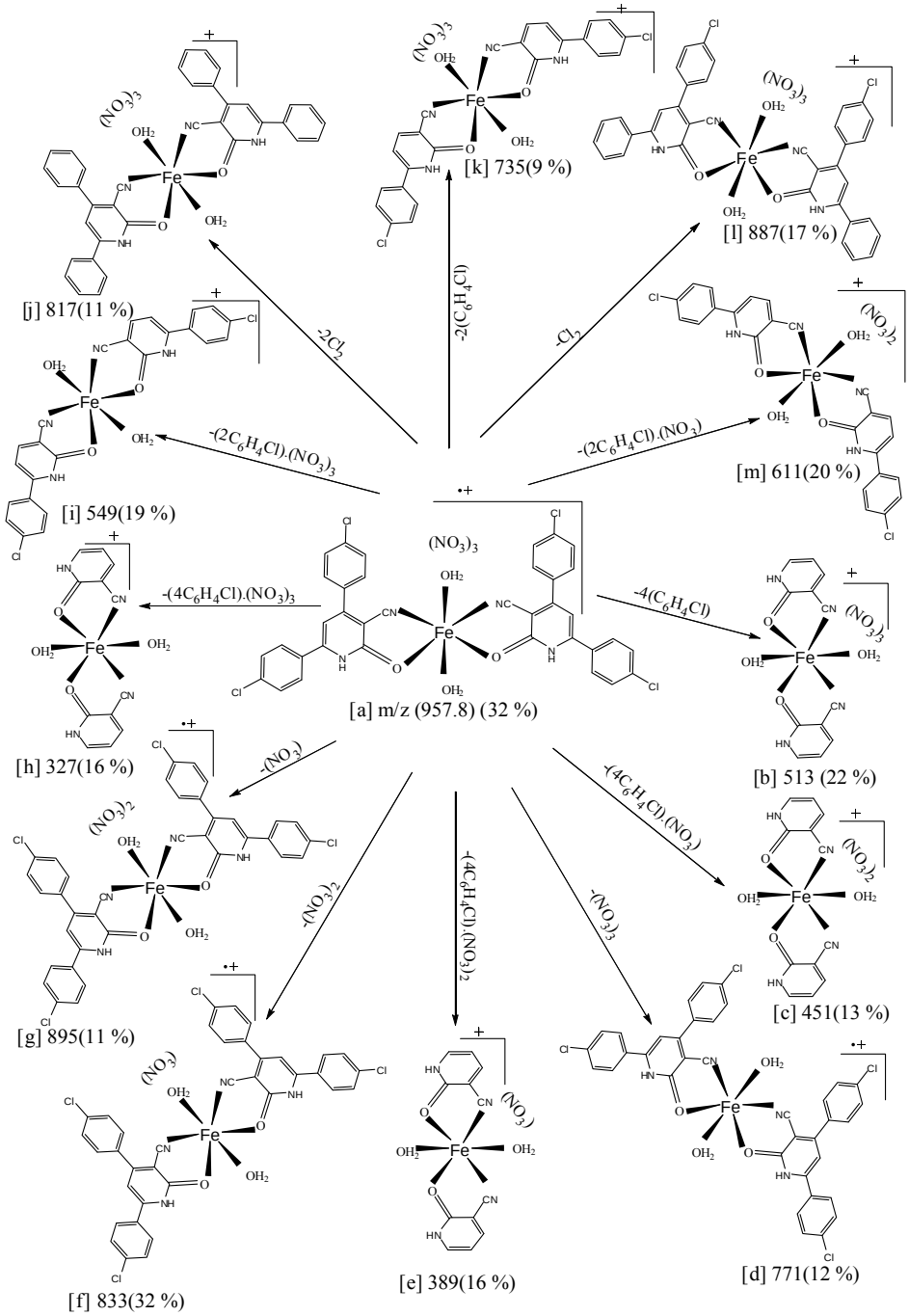

Scheme 4. Fragmentation pattern of $[Fe(L)_2(H_2O)_2](NO_3)_3$.

Thermal analysis

The 4,6-bis (4-chlorophenyl)-2-oxo-1,2-dihydropyridine-3-carbonitrile (L) of Mn(II), Fe(III), Co(II) and Ni(II) complexes are stable at room temperature and can be stored for several months without any changes. To establish the proposed formulae for the new complexes of Mn(II), Fe(III), Co(II) and Ni(II) under investigation, thermogravimetric (TGA) and differential thermogravimetric (DTG) analyses were carried out for the solid complexes under N_2 flow from ambient temperature to 800 ^oC (Figure 5). Table 5 give the maximum temperature values, $T_{max}/^oC$ together with the corresponding weight loss for each step of the decomposition reactions of the above compounds. The obtained data strongly support the proposed chemical formulae of the compounds and indicated that the ligand (L) is thermally stable at room temperature. Decomposition of the L started at 350 ^oC and finished at 600 ^oC with one stage at maximum 411 ^oC and is accompanied by a weight loss of 82.50% corresponding to loss of five molecules of acetylene, one molecule of carbon monooxide and two molecule of cyanogen chloride [21].

The thermal decomposition of Mn(II), Fe(III) and Co(II) complexes proceed approximately with one main degradation step at 200 and 360 ^oC for Mn(II), at 320 ^oC for Fe(III) and at 502 ^oC for Co(II) leaving $MnSO_4$, Fe_2O_3 and CoO as a final products (Table 5).

The TGA curve of $[Ni(L)(H_2O)_2]SO_4.6H_2O$ shows two stages of decomposition. The first stage occurs at maximum temperature 80 ^oC corresponds to the loss of six water molecules with mass loss of 11.56% (calc. 11.01%). The relatively low value of temperature of this step may indicated that these water molecules undergoes less H-bonding. The second step of decomposition occurs at two maxima at 337 and 451 ^oC, is accompanied by a weight loss of 91.51% which leaving NiO+3C, as resdue [22, 23].

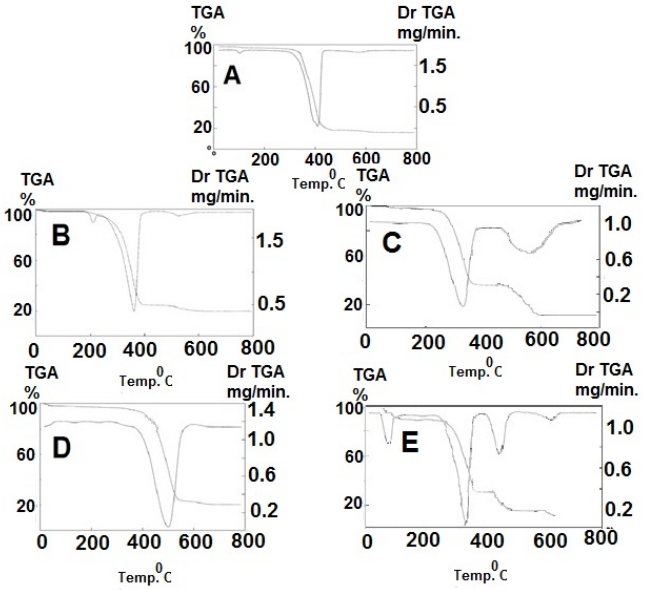

Figure 5. TGA and DTG curves of (A) 4,6-bis (4-chlorophenyl)-2-oxo-1,2-dihydropyridine-3-carbinitrile (L), (B) $[Mn(L)_2(H_2O)_2]SO_4$, (C) $[Fe(L)_2(H_2O)_2](NO_3)_3$, (D) $[Co(L)_2(H_2O)_2]Cl_2$ and (E) $[Ni(L)_2(H_2O)_2]SO_4.6H_2O$.

Table 5. The maximum temperature T_{max} (^oC) and weight loss values of the decomposition stages for L_2, Mn(II), Fe(III), Co(II) and Ni(II).

Compounds	Decomposition	T_{max} (^oC)	Weight loss (%)		Lost species
			Calc.	Found	
(L)	First step	411	82.50	82.50	$5C_2H_2 + CO + 2NCCl$
($C_{18}H_{10}N_2OCl_2$)	Total loss		82.50	82.50	
	Residue		17.50	17.50	5C
$[Mn(L)_2(H_2O)_2]SO_4$	First step	200, 360	77.11	79.43	$12C_2H_2 + 4CO + 4NCCl$
($C_{36}H_{24}N_4O_8Cl_4SMn$)	Total loss		77.11	79.43	
	Residue		22.89	20.56	$MnSO_4 + 4C$
$[Fe(L)_2(H_2O)_2](NO_3)_3$	First step	320	94.18	94.40	$11C_2H_2 + NO + 10CO + 0.5H_2O + 4NCCl + 0.5H_2$
($C_{36}H_{24}N_7O_{13}Cl_4Fe$)	Total loss		94.18	94.40	
	Residue		5.81	5.60	$0.5Fe_2O_3$
$[Co(L)_2(H_2O)_2]Cl_2$	First step	502	82.65	82.50	$12C_2H_2 + 0.5N_2 + 3CO + 1.5Cl_2 + 3NCCl$
($C_{36}H_{28}N_4O_6Cl_6Co$)	Total loss		82.65	82.50	
	Residue		17.34	17.50	$CoO + 6C$
$[Ni(L)_2(H_2O)_2]SO_4.6H_2O$	First step	80	11.01	11.65	$6H_2O$
($C_{36}H_{30}N_4O_{11}Cl_4SNi$)	Second step	337, 451	80.56	79.95	$12C_2H_2 + 5CO + SO_2 + 4NCCl$
	Total loss,		91.57	91.51	$NiO + 3C$
	Residue		8.43	8.49	

Table 6. The inhibition diameter zone values (mm) for (L_2) and its metal complexes.

Compounds		Microbial species					
		Bacteria				*Fungi*	
		E. coli	*P. aeruginosa*	*B. subtilis*	*S. aureus*	*C. albuicans*	*A. fumigates*
(L_2)		11±0.10	9±0.33	13±0.04	15±0.07	17±0.55	18±0.08
L_2 / Mn(II)		18^{+2}±0.10	17^{+2}±0.33	18^{+1}±0.04	19^{+1}±0.07	19^{NS}±0.55	19^{NS}±0.08
L_2 / Fe(III)		19^{+2}±0.10	19^{+3}±0.33	19^{+1}±0.04	20^{+1}±0.07	18^{NS}±0.55	20^{NS}±0.08
L_2 / Co(II)		20^{+2}±0.10	20^{+3}±0.33	21^{+2}±0.04	22^{+2}±0.07	20^{+1}±0.55	22^{+1}±0.08
L_2 / Ni(II)		19^{+2}±0.10	21^{+3}±0.33	20^{+2}±0.04	20^{+1}±0.07	21^{+1}±0.55	26^{+2}±0.08
$Fe(NO_3)_3.9H_2O$		10±0.33	12±0.11	0	0	0	0
$CoCl_2.6H_2O$		0	0	0	0	0	0
$NiSO_4.6H_2O$		0	0	0	0	0	0
$MnSO_4.6H_2O$		0	0	0	0	0	0
Control (DMSO)		0	0	0	0	0	0
Standard	Ampicilin	0	0	28±0.40	0	0	0
	Amoxycilin	0	0	22±0.11	18±1.73	0	0
	Cefaloxin	24±0.34	0	27±1.15	16±0.52	0	0

ND: non-detectable. i.e., the inhibition zones exceed the plate diameter. Statistical significance P^{NS} P not significant, P >0.05; P^{+1} P significant, P < 0.05; P^{+2} P highly significant, P < 0.01; P^{+3} P very highly significant, P < 0.001; student's-test (paired).

Antimicrobial activity

The efficiencies of L and their metal complexes have been investigated against two Gram-negative, *Escherichia coli* and *Pseudomonas aeruginosa* and two Gram-positive, *Staphylococcus aureus* and *Bacillus subtilis* also antifungal screening was studied against two species *Aspergillus fumigatas* and *Candida albicans* microorganisms. The results of the antibacterial study of L and their complexes (Table 6) have inhibitory action against all four

types of bacteria and antifungal activity (Figure 6). The complexes of Mn(II) shows a highly significant against *Escherichia coli* and *Pseudomonas aeruginosa* and moderate activity against *Bacillus subtilis*, *Staphylococcus aureus* than free ligand. Fe(III) shows very highly significant against *Pseudomonas aeruginosa*, a highly significant against *Escherichia coli* and moderate significant against Gram-positive. The Co(II) shows very high significant against *Pseudomonas aeruginosa* and highly significant against *Escherichia coli*, *Staphylococcus aureus* and *Bacillus subtilis* and moderate significant for antifungal species. For Ni(II) complex shows very highly significant against *Pseudomonas aeruginosa* but, for *Escherichia coli*, *Bacillus subtilis* and *Aspergillus fumigates* are highly significant and moderate significant against *Staphylococcus aureus* and *Candida albicans*. The nature of the metal ion coordinated to a drug may have a significant role to this diversity. In general for metal complexes showing antimicrobial activity, the following five principal factors [13, 14] should be considered: i) the chelate effect; ii) the nature of the ligands; iii) the total charge of the complex; iv) the nature of the ion neutralizing the ionic complex; and v) the nuclearity of the metal center in the complex.

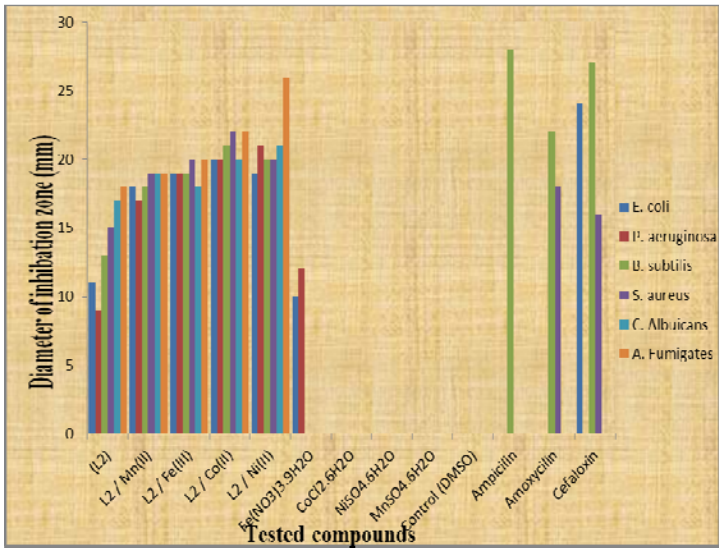

Figure 6. Statistical representation for biological activity of (L_2) and its metal complexes.

Computational details

Computational method

The geometric parameters and energies were computed by DFT at the B3LYP/CEP-31G level, using the GAUSSIAN 98W package of the programs, on geometries that were optimized at CEP-31G basis set. The high basis set was chosen to detect the energies at a highly accurate level. The atomic charges were computed using the natural atomic orbital populations. The B3LYP is the keyword for the hybrid functional, [24], which is a linear combination of the gradient functional proposed by Becke [25] and Lee *et al.* [26] together with the Hartree-Fock local exchange function [27].

Structural parameters and models

(4,6)bis-4-chlorophenyle-2-oxo-1,2-dihydropyridine-3-carbonitrile (L)

The biological activity of pyridinones L is mainly determined by its fine structure, the L has many characteristic structural features. The molecule is not highly sterically-hindered, the two benzene rings in the same plane of the pyridinone ring. This observation is supported by the values of calculated dihedral angles of C3C4C5C8 and C6C5C8C9 are 180.00˚ and 0.00˚ (Table 7) while the dihedral angles of C11C17C21C22 and C11C17C18C19 are 180.00˚and 180.00˚. Scheme 5 shows the optimized geometrical structure of L molecule, the dihedral angles of N16C15C9C13 and N16C15C9C8 are 0.00˚ and 180.00˚ which confirms –CN group in the same plane of molecule.

The bond distance of C13-O14 is 1.289Å and the bond angle of C9C15N16 is 164.29˚ reflects on sp hybridization of C15 and the bond length of C15N16 is 1.208Å. The values of bond distances are compared nicely with that obtained from experimental data [28].

There is a significant built up of charge density on oxygen atom and two nitrogen atoms of pyridinone and cyano group, so L is bi-dentate ligand (O14 and N16 atoms) and the molecule is not highly dipole μ = 7.37 because the planarity of L molecule. The charge accumulated on Cl7and Cl23 are -0.287 and -0.277, respectively, also, the charge on N12 and N16 are -0.218 and -0.258, respectively. The total energy of the optimized geometry of L molecule is -191.782 au. The metal ligand binding, dipole moment, total energy and optimized geometrical structure of all complexes were studied and the DFT of Mn(II) complex is used as example in my article.

Table 7. Equilibrium geometric parameters bond lengths (Å), bond angles (˚), dihedral angles (˚) and charge density of (4,6)bis-4-chlorophenyle-2-oxo-1,2-dihydropyridine-3-carbinitrile ligand by using DFT/B3LYP/Cep-31G.

Bond length (Å)			
C13-O14	1.289 (1.30)	C8-C10	1.426 (1.47)
C10-C11	1.377 (1.38)	C15-C16	1.208 (1.29)
C9-C15	1.428 (1.41)	C11-N12	1.385
C13-N12	1.393	C8-C9	1.387 (1.38)
Bond angle (˚)			
C9C15N16	164.29	C9C13O14	128.68
C3C1Cl7	117.62	C2C1Cl7	118.03
C19C20Cl23	118.07	C17C11N12	116.24
C5C8C9	118.80	C4C5C8	124.36
C9C13O14	128.68	C12C13O14	116.25
C11C17C18	121.35	C22C20Cl23	118.02
Dihedral angles (˚)			
C3C4N5C8	180.00	C4C5C8C9	180.00
C6C5C8C9	0.00	C11C17C18C19	180.00
C13C9C15N16	0.00	C22C21C17C11	180.00
C2C6C5C8	180.00	N16C15C9C8	180.00
Charges			
C15	0.147	Cl7	-0.287
N16	-0.258	Cl23	-0.227
C13	0.390	C1	0.246
O14	-0.449	C20	0.249
N12	-0.218		
Total energy/au			-191.782
Total dipole moment/D			7.37

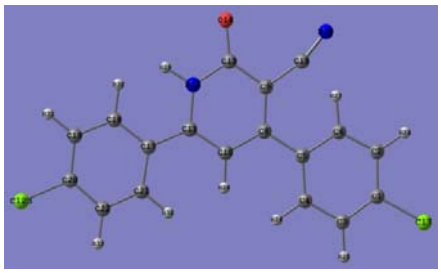

Scheme 5. The optimized geometrical structure of L by using B3LYP/CEP-31G.

The Mn(II) L complexes

Mn(II) binds two molecules of L through two oxygen and two nitrogen atoms of L. The complex is six-coordinate with four coordinate bonds from two L molecules and water or sulfate. We studied $[Mn(L)_2(SO_4)]$ and $[Mn(L)_2(H_2O)_2]^{2+}$.

Description of the structure of $[Mn(L)_2(SO_4)]$

The structure of complex with atomic numbering scheme is shown in Scheme 6. The complex is six-coordinate with distorted octahedral environment around the metal ion. The Mn(II) is coordinated through two oxygen and two nitrogen atoms of two ligand and two oxygen atoms of SO_4^{-2} group. The Mn-O25 and Mn-O33 bond lengths are 2.026 Å and 2.025 Å, respectively [29, 30]. The Mn-N27 and Mn-N29 are 1.795 Å and 1.796 Å, respectively, (Table 8) and the bond distance between Mn-O2 and Mn-O3 of sulfate group are 1.849 Å and 1.849 Å, respectively [31]. Also, the angles around the Mn (II) with surrounding four oxygen atoms and two nitrogen atoms vary from 73.46˚ to 172.31˚; these values differ legally from these expected for a regular octahedron.

The energy of this complex is -434.252 au while the dipole moment is lower than free ligand 4.425D also, the charge accumulated on O25 and N27 of the first molecule are -0.396 and -0.179, respectively. O33 and N29 of the second molecule are -0.386 and -0.193, respectively. The bond angle of O4SO5 of sulfate group is 130.76˚ [32].

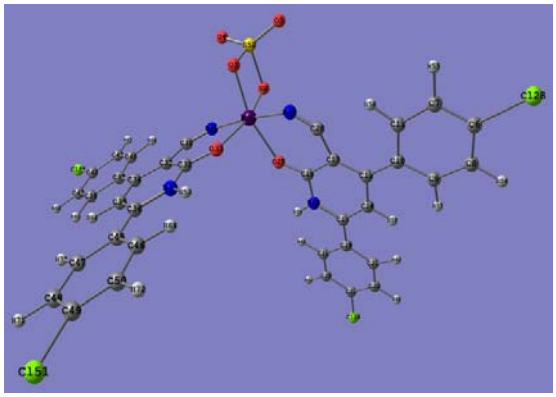

Scheme 6. Optimized geometrical structure of $[Mn(L)_2(SO_4)]$ complex by using B3LYP/CEP-31G.

Table 8. Equilibrium geometric parameters bond lengths (Å), bond angles (˚) and charge density of [Mn $(C_{18}H_{10}N_2OCl_2)_2(SO_4)$] by using DFT/B3LYP/Cep-31G.

Bond length (Å)			
Mn-O25	2.016	C15-O25	1.253
Mn-N27	1.795	C32-O33	1.253
Mn-O33	2.015	C26-N27	1.145
Mn-N29	1.796	C30-N29	1.145
Mn-O2	1.849	S-O2	1.652
Mn-O3	1.849	S-O3	1.651
Bond angle (˚)			
O25 Mn N27	73.46	O25 Mn O33	96.07
O25 Mn N29	102.27	N27 Mn N29	172.31
O3 Mn N27	90.74	O2 Mn N29	91.52
O2 Mn O3	77.14	O3 Mn O33	95.80
O3 Mn N29	94.42	O25 Mn O3	161.71
O2 Mn O25	94.81	O2 Mn N27	95.19
N27 Mn O33	100.34	O2 Mn O33	163.06
		N29 Mn O33	73.48
Charges			
Mn	0.343	O2	-0.353
O25	-0.396	O3	-0.302
N27	-0.179	C15	0.466
O33	-0.386	C32	0.468
N29	-0.193		
Total energy/au			-434.252
Total dipole moment/D			4.425

Description of the structure of $[Mn(L)_2(H_2O)_2]^{2+}$

The structure of complex with atomic numbering scheme is shown in Scheme 7. The complex consists of two units of L molecule and two water molecules with Mn(II). The complex is six-coordinate with distorted octahedral environment around the metal ion. The Mn(II) is coordinated to one O_{keto} atom and one N_{car} atom of L ligand and two oxygen atoms for water. The total energy of this complex is obtained by using density functional theory combined with B3LYP/CEP-31G as basis set. The bond angle between O22MnO30 is 96.07 and also the angle between N24MnN26 is 164.18˚ (Table 9) so the two L molecules are not lying in the same plane they are perpendicular respect to each other with angle equal 90˚. The angle between O2MnO49 is 91.04˚ this value reflects that the two water molecules not in trans-form respect to each other but they are lying in cis-form and then they are perpendicular to each other.

The bond length between Mn-O30 and Mn-O22 are 2.026 Å and 2.025 Å are longer than that Mn-N26 and Mn-N24 (1.799 Å and 1.800 Å) [29-31], while the bond distance between Mn-O_{H2O} vary from 1.845 Å and 1.846 Å [32, 33]. Also, the angles around Mn(II) with surrounding oxygen atoms vary from 73.44˚ to 166.15˚; these values agree with these expected for a distorted octahedron.

The bond distances between Mn(II) and surrounded oxygen atoms and nitrogen atoms of L in water complex are shorter than that in sulfate complex. Also, the charge accumulated on O_{keto} (-0.396 and -0.386) and N_{car} (-0.179 and -0.193), in sulfate complex while, O_{keto} (-0.415 and -0.421) and N_{car} (-0.207 and -0.205), in water complex. There is a strong interaction between Mn (II) which become has charge equal +0.546 in case of water complex while, in case of sulphate complex the charge accumulated on Mn(II) is 0.343. The energy of the water complex is more negative than sulfate complexes -474.816 au and relatively weak dipole 7.425D. For all these reasons the water complex is more stable than other complexes and Mn(II) favor

coordinated with two molecules of water more than one molecule of sulfate ion to complete the octahedron structure.

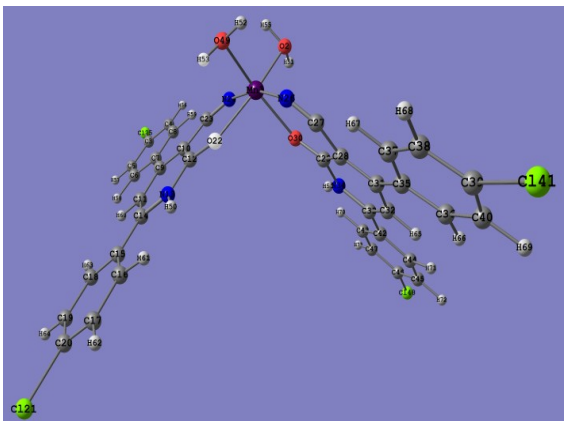

Scheme 7. Optimized geometrical structure of $[Mn(L)_2(H_2O)_2]^{2+}$ complex by using B3LYP/CEP-31G.

Table 9. Equilibrium geometric parameters bond lengths (Å), bond angles (˚) and charge density of [Mn $(C_{18}H_{10}N_2OCl_2)_2(H_2O)_2]^{2+}$ by using DFT/B3LYP/Cep-31G.

Bond length (Å)			
Mn-O30	2.026	C29-O30	1.253
Mn-N24	1.80	C12-O22	1.252
Mn-O22	2.025	C29-N34	1.363
Mn-N26	1.799	C23-N24	1.146
Mn-O2	1.845	C29-C28	1.378
Mn-O49	1.846	C10-C12	1.378
Bond angle (˚)			
O30 Mn N26	73.49	O20 Mn O2	91.05
O49 Mn N26	91.42	O22 Mn O2	166.15
O30 Mn N24	96.26	N24 Mn O49	98.57
O22 Mn N24	73.44	N26 Mn O22	94.42
N24 Mn O2	92.74	O30 Mn O22	91.33
N26 Mn N24	164.18	O30 Mn O49	164.91
N26 Mn O2	99.35	O22 Mn O49	90.12
		O2 Mn O49	91.05
Charges			
Mn	0.546	O2	-0.325
O30	-0.421	O49	-0.333
N26	-0.205	C29	0.453
O22	-0.415	C12	0.454
N24	-0.207		
Total energy/au			-474.816
Total dipole moment/D			7.425

REFERENCES

1. Rashad, A.E.; Shamroukh, A.H.; El-Hashash, M.A.; El-Farargy, A.F.; Yousif, N.M.; Salama, M.A.; Mostafa, A.; El-Shahat, M. *J. Heterocycl. Chem.* **2012**, 49, 1130.
2. Katritzky, A.R.; Taylor, R. *Adv. Heterocycl. Chem.* **1990**, 47, 308.
3. Jasinski, J.P.; Butcher, R.J.; Narayana, B.; Veena, K.; Yathirajan, H.S. *Acta Cryst.* **2009**, E65, 2641.
4. Zordok, W.A.; Sadeek, S.A.; EL-Shwiniy, W.H. *J. Coord. Chem*. **2012**, 65, 353.
5. Frisch, M.J.; Trucks, G.W.; Schlegel, H.B.; Scuseria, G.E.; Robb, M.A.; Cheeseman, J.R.; Zakrzewski, V.G.; Montgomery, J.A.; Stratmann, R.E.; Burant, J.C.; Dapprich, S.; Millam, J.M.; Daniels, A.D.; Kudin, K.N.; Strain, M.C.; Farkas, O.; Tomasi, J.; Barone, V.; Cossi, M.; Cammi, R.; Mennucci, B.; Pomelli, C.; Adamo, C.; Clifford, S.; Ochterski, J.; Petersson, G.A.; Ayala, P.Y.; Cui, Q.; Morokuma, K.; Malick, D.K.; Rabuck, A.D.; Raghavachari, K.; Foresman, J.B.; Cioslowski, J.; Ortiz, J.V.; Stefanov, B.B.; Liu, G.; Liashenko, A.; Piskorz, P.; Komaromi, I.; Gomperts, R.; Martin, R.L.; Fox, D.J.; Keith, T.; Al-Laham, M.A.; Peng, C.Y.; Nanayakkara, A.; Gonzalez, C.; Challacombe, M.; Gill, P.M.W.; Johnson, B.; Chen, W.; Wong, M.W.; Andres, J.L.; Gonzalez, C.; Head-Gordon, M.; Replogle, E.S.; Pople, J.A. *Gaussian 98, Revision A.6*, Gaussian, Inc. : Pittsburgh PA; **1998**.
6. Stevens, W.J.; Krauss, M.; Bosch, H.; Jasien, P.G. *Can. J. Chem*. **1992**, 70, 612.
7. Vogel, A.I.; Tatchell, A.R.; Furnis, B.S.; Hannaford, A.J.; Smith, P.W.G. *Vogel Textbook of Practical Organic Chemistry*, Prentice Hall: London; **1996**; pp 88-90.
8. Beecher, D.J.; Wong, A.C. *Appl. Environ. Microbial*. **1994**, 60, 1646.
9. Fallik, E.; Klein, J.; Grinberg, S.; Lomaniee, C.E.; Lurie, S.; Lalazar, A. *J. Econ. Entomol*. **1993**, 77, 985.
10. Geary, W.J. *Coord. Chem. Rev*. **1971**, 7, 81.
11. King, D.E.; Malone, R.; Lilley, S.H. *Am. Fam. Phys*. **2000**, 61, 2741.
12. Nakamoto, K. *Infrared and Raman Spectra of Inorganic and Coordination Compounds*, 4th ed., Wiley: New York; **1988**, pp 139, 141.
13. Nour, E.M.; Taha, A.A.; Anaimi, I.S. *Inorg. Chem. Acta* **1988**, 139, 141.
14. Syamal, A.; Singhal, P.O.; Banerjee, S. *Synth. React. Inorg. Met.-Org. Chem.* **1980**, 10, 243.
15. Efthimiadou, E.K.; Katsarou, M.; Sanakis, Y.; Raptopoulou, C.P.; Karaliota, A.; Katsaros, N.; Psomas, G. *J. Inorg. Biochem*. **2006**, 100, 1378.
16. Zordok, W.A.; EL-Shwiniy, W.H.; EL-Attar, M.S.; Sadeek, S.A. *J. Mol. Struct*. **2013**, 1047, 267.
17. Turel, I. *Coord. Chem. Rev*. **2002**, 27, 232.
18. Nakamoto, K.; Mccarthy, P.J.; Fujiwara, S.; Shimura, Y.; Fujita, J.; Hare, C.R.; Saito, Y. *Spectroscopy and Structure of Metal Chelate Compounds*, John Wiley and Sons: New York; **1968**.
19. Cotton, F.A.; Wilkinson, G.; Murillo, C.A.; Bochmann, M. *Advanced Inorganic Chemistry*, 6th ed., Wiley: New York; **1999**.
20. Skauge, T.; Turel, I.; Sletten, E. *Inorg. Chem. Acta* **2002**, 247, 339.
21. David, L.R. *Handbook of Chemistry and Physics*, 87th ed., CRC Press: United Kingdom; **2006**.
22. Tagawa, H. *Thermochim. Acta* **1984**, 80, 23.
23. Poston, J.A.; Ranjani, V.; Siriwadane, Edward, Fisher, P.; Angela, Miltz, L. *App. Surf. Sci*. **2003**, 214, 83.
24. Kohn, W.; Sham, L.J. *Phys. Rev A* **1965**, 140, 1133.
25. Becke, A.D. *Phys. Rev. A* **1988**, 38, 3098
26. Lee, C.; Yang, W.; Parr, R.G. *Phys. Rev B* **1988**, 37, 785.
27. Flurry Jr., R.L. *Molecular Orbital Theory of Bonding in Organic Molecules*, Marcel Dekker: New York; **1968**.

28. Turel, I.; Golic, L.; Bukovec, P.; Gubina, M. *J. Inorg. Biochem*. **1998**, 71, 53.
29. Becker, T.M.; Krause Bauer, J.A.; Homrighausen, C.L.; Orchin, M. *J. Organomet. Chem*. **2000**, 602, 97.
30. Schlieife, F.; Rodenstein, A.; Kirmse, R.; Kersting, B. *Inorg. Chim. Acta* **2011**, 374, 521.
31. Kajnakova, M.; Cernak, J.; Kavecansky, V.; Gerared, F.; Papageorgiou, T.; Orendac, M.; Orendacova, A.; feher, A. *Sol. Stat. Sci*. **2006**, 8, 203.
32. Gudasi, K.B.; Patil, S.A.; Vadavi, R.S.; Shenoy, R.V.; Nethaji, M.; Bligh, S.W.A. *Inorg. Chem. Acta* **2006**, 359, 3229.
33. Bermejo, M.R.; Fondo, M.; García-Deibe, A.; González, A.M.; Sousa, A.; Sanmartín, J.; McAuliffe, C.A.; Pritchard, R.G.; Watkinson, M.; Lukov,V. *Inorg. Chem. Acta* **1999**, 293, 210.